ChemElectroChem

Research Article
doi.org/10.1002/celc.202101720

Chemistry Europe
European Chemical Societies Publishing

www.chemelectrochem.org

Special Collection

Electrochemical Treatment of Synthetic Wastewaters Contaminated by Organic Pollutants at Ti_4O_7 Anode. Study of the Role of Operative Parameters by Experimental Results and Theoretical Modelling

Yongyong Hao,[a, b] Pengfei Ma,[b, c] Hongrui Ma,[a] Federica Proietto,[b] Claudia Prestigiacomo,[b] Alessandro Galia,[b] and Onofrio Scialdone*[b]

In the last years, an increasing attention has been devoted to the utilization of anodic oxidation (AO) technologies for the treatment of wastewater polluted by recalcitrant organics. Recently, Ti_4O_7 was proposed as a promising anode for AO for the treatment of various organics. Here the potential utilization of commercial Ti_4O_7 anodes has been evaluated considering the electrochemical treatment of synthetic wastewater contaminated by three very different organic molecules (namely, oxalic acid, phenol and Acid Orange 7), all characterized by a very high resistance to AO. The performances of Ti_4O_7 were compared with that of two largely investigated anodes: Boron-doped diamond (BDD), which is probably the most effective electrode for AO, and an Ir-based anode which presents a relatively low cost. Moreover, the effect of various operative conditions (current density, mixing rate and initial concentration of the organic) was evaluated by both experimental studies and the adoption of a theoretical model previously developed for BDD anodes. It was shown that the performances of the process can be improved by a proper selection of operative conditions. Moreover, it was found that the proposed model can be effectively used to predict the effect of operative parameters at Ti_4O_7 anodes, thus helping the process optimization.

Introduction

In the last years, several researchers have studied the implementation of innovative advanced oxidation processes (AOPs) for the effective treatment of wastewater contaminated by organic pollutants resistant to conventional biological processes. Some electrochemical processes such as anodic oxidation (AO),[1–5] oxidation by electro-generated active chlorine[1,2,6,7] and electro-Fenton (EF)[1,2,8,9] gave very promising results in terms of high removals of organics using an environmental friend reagent such as the electron and mild conditions such as room temperature and pressure close the atmospheric one. Moreover, it was shown that the electrochemical treatment of wastewater can use electric energy from renewable energies such as salinity gradients[10,11] and/or it can be coupled with other redox processes, such as carbon dioxide reduction,[12] thus strongly improving the economic perspectives of such process. AO consists in the oxidation of organics by (*i*) direct electron transfer to the anode, which yields very poor decontamination, and (*ii*) reaction with electrogenerated oxidants generated from water oxidation at the anode surface, such as physically adsorbed hydroxyl radical (•OH) or chemisorbed active oxygen (i.e., oxygen in the lattice of a metal oxide anode (MO)).[1] The action of these oxidizing compounds, whose formation depends on the nature of the anode, give total or partial oxidation of organics, respectively. Boron doped diamond (BDD) thin-film is considered the best anode material for AO due to its high chemical stability and large generation of very reactive hydroxyl radicals that ensures complete mineralization of many organic pollutants.[1–3,13,14] On the other hand, the utilization of BDD on large-scale applications was limited up to now by its high cost.[1,13] The utilization of many other anodes has been also limited by short service life, as in the case of Ti/SnO_2-based electrodes, risk of contamination by chemical leaching (such as for PbO_2) or slow mineralization of organics coupled with low current efficiency (for many anodes including IrO_2- and RuO_2-based ones).[1,2]

In the last years, ceramic electrodes based on sub-stoichiometric titanium oxides and, in particular, Ti_4O_7 have been proposed as quite promising anodes for AO for the treatment of various organics, such as trichloroethylene,[15] dichloroethane,[16] phenol,[17] amoxicillin,[18] paracetamol,[19] poly- and perfluoroalkyl substances[20] and tetracycline.[21] Moreover,

[a] Dr. Y. Hao, Prof. H. Ma
School of Environmental Science and Engineering
Shaanxi University of Science & Technology
Xi'an 710021, P.R. China
[b] Dr. Y. Hao, Dr. P. Ma, Dr. F. Proietto, Dr. C. Prestigiacomo, Prof. A. Galia, Prof. O. Scialdone
Dipartimento di Ingegneria
Università degli Studi di Palermo
Viale delle Scienze, Ed. 6, Palermo 90128, Italy
E-mail: onofrio.scialdone@unipa.it
[c] Dr. P. Ma
Department of Chemical Engineering
Taiyuan University of Technology
Taiyuan 030024, P.R. China

Special Collection
An invited contribution to the Retiring Board Members Special Collection

Zaky and Chaplin have shown that *p*-substituted phenol can be oxidized at a Ti_4O_7 reactive electrochemical membrane,[22] while the group of Oturan has shown that the Ti_4O_7 anode can be used also for EF treatment.[23]

The Ti–O system belongs to Magneli phases homologous series with the empirical formula Ti_nO_{2n-1} ($n \geq 3$) and many of these oxides exhibit high electrical conductivity at room temperature, good corrosion resistant and high chemical stability.[24] Hydroxyl radicals were detected at Ti_4O_7 under anodic polarization using a spin trap (4-POBN).[15] Moreover, Bejan and co-authors have reported that, at BDD, hydroxyl radicals show a similar, but not identical, reactivity to that of free •OH(aq), while, at Ebonex, a conductive ceramic material of approximate composition Ti_4O_7, the hydroxyl species appears to be less abundant but more reactive than at BDD.[25]

In the present work, the AO at commercial Ti_4O_7 anode was investigated with the main aim to evaluate the role of various operative parameters, including current density, mixing rate and concentration of the organic pollutant. Oxalic acid (OA) was used as a model organic pollutant for its high resistance to AO.[26–31] The effect of the nature of the organic was also studied by evaluating the treatment of synthetic solutions of other two very different but rather resistant organics, such as phenol and Acid Orange 7 (AO7), whose abatement was previous investigated at different anodes.[17,32,33] Moreover, the performances of Ti_4O_7 were compared with that of two widely investigated anodes such as BDD, which is characterized for the very high removal of organics but high capital costs and cell potentials, and Ti/IrO_2–Ta_2O_5 which presents relatively low cost and high stability but lower abatements, in order to assess the potential utilization of this material for the treatment of wastewater contaminated by organic pollutants. Eventually, the electrochemical results were compared with the predictions of a theoretical model in order to better understand the process and to develop a mathematical tool that can be used to predict the effect of other operating conditions and to assist the scale-up process. Various models were proposed in the last years for AO including that developed by the groups of Comninellis,[34] Rodrigo,[35] Polcaro[36] and Scialdone.[37–39] In particular, in this work, we will use a rather simple theoretical model proposed in the last years by some of the authors that was able to predict the effect of numerous operative parameters for both metal oxides such as Ti/IrO_2–Ta_2O_5[38] and BDD.[37,39]

Results and Discussion

Effect of the nature of the anode

Some preliminary experiments were performed in an undivided cell equipped with different anodes (Ti_4O_7, BDD and Ti/IrO_2–Ta_2O_5) and a Ni cathode with magnetic stirring (300 rpm) under galvanostatic conditions using an aqueous solution of the model organic pollutant OA (30 mM) and Na_2SO_4 as supporting electrolyte. A quite low current density *j* (5 mA cm^{-2}) was selected in order to have an oxidation process not kinetically limited by the mass transfer of OA to the anodic surface.

As shown in Figure 1, a strong effect of the nature of the anode on the abatement of OA (X_{OA}), current efficiency (*CE*) and instantaneous current efficiency (*ICE*) was observed.

After 13 hours (corresponding to 1170 C), X_{OA} was 65, 80 and 98% at Ti/IrO_2–Ta_2O_5, Ti_4O_7 and BDD, respectively, as a

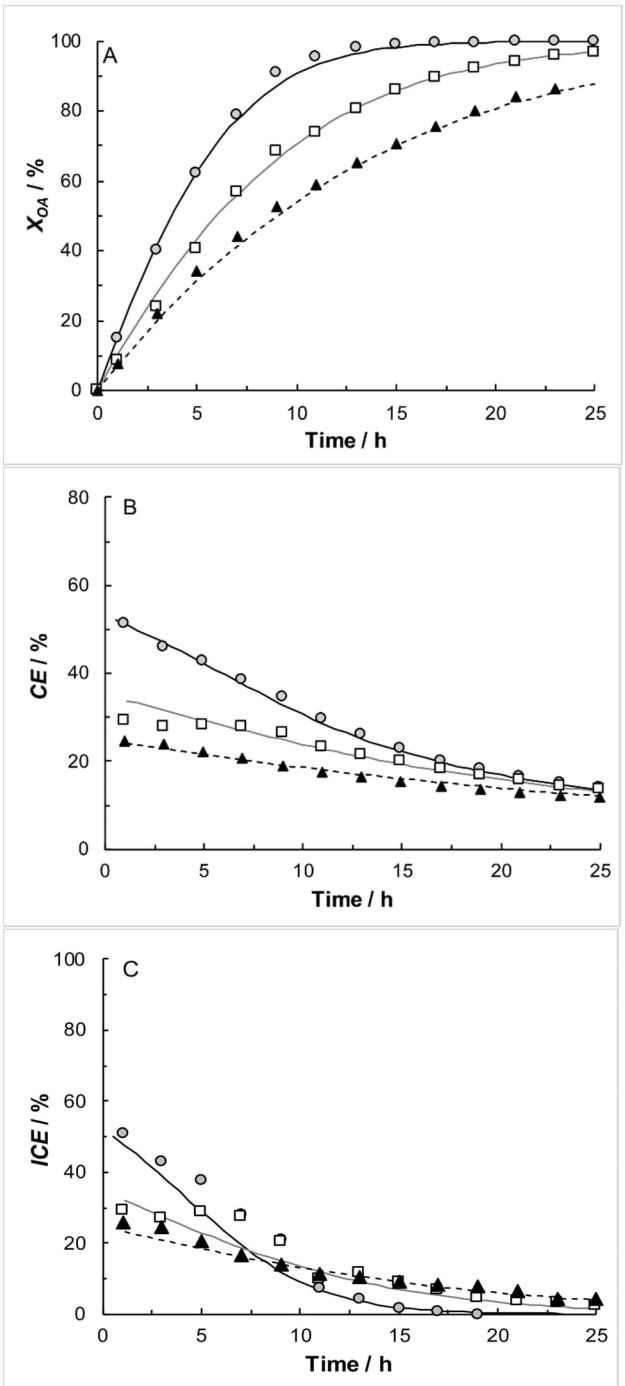

Figure 1. Effect of the nature of the anode: BDD (●), Ti_4O_7 (□) or Ti/IrO_2–Ta_2O_5 (▲) on the X_{OA} (%) (1 A), *CE* (%) (1B) and *ICE* (%) (1 C).Electrolyses of a solution of OA (30 mM), Na_2SO_4 (50 mM) (pH 2) were performed at 5 mA cm^{-2} and 300 rpm. Ni was used as cathode. Theoretical curves (lines) obtained by Eq. (6) with the parameters *[RH]** reported in Table 1.

result of quite different current efficiencies achieved for the three anodes (16, 20 and 25%, respectively). However, after 21 hours (corresponding to 1890 C) similar X_{OA} and *CE* were achieved at BDD (99%) and Ti_4O_7 (94%), while Ti/IrO_2–Ta_2O_5 gave a lower X_{OA} close to 84%. The different results obtained at the three tested anodes can be ascribed to the different nature and abundance of generated hydroxyl radicals. In particular, at metal oxide electrodes, according to the literature, water oxidation gives rise to adsorbed hydroxyl radicals (Eq. (1)) which can potentially evolve towards the formation of chemisorbed oxygen (Eq. (2)) or oxygen evolution (Eq. (3)).

Chemisorbed oxygen can at its turn evolve towards oxygen evolution according to Eq. (4). Oxidizable organics can, as a consequence, be potentially oxidized by adsorbed hydroxyl radicals (Eq. (5)), by adsorbed oxygen or by both these paths. In particular, Comninellis[40] proposed that adsorbed oxygen gives rise to a less effective and partial oxidation process while physisorbed hydroxyl radicals favor the complete combustion of organics.

$$MO_x + H_2O \rightarrow MO_x(^{\bullet}OH) + H^+ + e^- \quad (1)$$

$$MO_x(^{\bullet}OH) \rightarrow MO_{x+1} + H^+ + e^- \quad (2)$$

$$MO_x(^{\bullet}OH) \rightarrow MO_x + 0.5O_2 + H^+ + e^- \quad (3)$$

$$MO_{x+1} \rightarrow MO_x + 0.5O_2 \quad (4)$$

$$MO_x(^{\bullet}OH) + RH \rightarrow MO_x + H_2O + \text{oxidation products} \quad (5)$$

In particular, for IrO_2-based anodes, the formation of chemisorbed oxygen, proven using labeled oxygen and mass spectrometry measurements,[41,42] justifies the slow removal of OA. Conversely, the very fast removal of OA at BDD is coherent with fact that this material gives rise to the formation of very reactive hydroxyl radicals that were assumed to be weakly physical adsorbed or even free to move in the aqueous phase.[1,2] In the case of Ti_4O_7, intermediate results were obtained probably due to the fact that this anode gives rise to the formation of •OH but in smaller amounts with respect to BDD.[25] It is worth to mention that similar results were reported by other scholars for the treatment of different organic compounds. As an example, although Ti_4O_7 anode provides a lesser mineralization rate for the treatment of aqueous solutions of amoxicillin compared to BDD, it exhibited better performances with respect to Pt and DSA.[18] In addition, from the applicative point of view, it is relevant to evaluate and compare the energetic consumption (EC) of the process. It was found that the utilization of Ti_4O_7 allows to perform the process with low values of EC and, as a consequence, low operating costs for the wastewater treatment. According to the data shown in Figure 1, after 13 hours, the EC per $Kg_{TOC\text{-}eq}$ was approximately 43, 37.8 and 35.7 kWh/$Kg_{TOC\text{-}eq}$ using Ti/IrO_2–Ta_2O_5, BDD and Ti_4O_7, respectively. While, by comparing the EC when each process reaches an X_{OA} close to 90%, the performances of the Ti_4O_7 were comparable or lower with respect to BDD or Ti/IrO_2–Ta_2O_5, respectively. In particular, to reach X_{OA} close to 90%, the EC was 35, 32 and 60 kWh/$Kg_{TOC\text{-}eq}$ using Ti_4O_7 after 19 h, BDD after 11 h and Ti/IrO_2–Ta_2O_5 after 25 h, respectively, as a result of the good performances of Ti_4O_7 in the removal of OA. This shows that Ti_4O_7 could be suitable also from an economic point of view for industrial application on the wastewater treatment plant.

The effect of the anode was also investigated by polarization curves and chronoamperometric measurements recorded both in the absence and in the presence of different concentrations of OA. As shown in Figure 2A and 2B, at both pH 2 and 12, at BDD anodes, the water discharge started at more positive working potentials with respect to the Ir-based anode. Ti_4O_7 presented an intermediate situation, thus showing that this anode gives an overpotential for oxygen evolution lower than BDD but higher than Ti/IrO_2–Ta_2O_5.

When OA was added to the water solution, the polarization curves shifted to less positive potentials at all adopted anodes (Figure 2A, 2B). In particular, current densities increased almost linearly with AO concentration at all adopted potentials at both pH 2 and 12 (Figure 2C, 2D). Similar results were obtained for the three anodes also by chronoamperometric measurements (Figure 3A, 3B). Please, consider that a similar trend was observed at BDD anodes for dilute solutions of various carboxylic acids.[14,43] For formic, maleic and succinic acids the linear increase of the current density with the concentration was attributed to their fast oxidation with hydroxyl radicals which annihilates their concentrations at the anode surface giving an expression of the total current density that depends on the mass transfer rate of organics for dilute solutions of these acids.[43] However, in the case of oxalic acid the potential occurrence of a direct anodic oxidation was also considered[14,43] since this molecule is considerably less reactive towards hydroxyl radicals with respect to the other carboxylic acids.[44] In the literature it was also observed that for various organics, including succinic and maleic acids, at high concentrations the current density did not depend on their concentrations as a probable result of adsorption phenomena.[43,45] However, as shown in Figure 2 and 3, for our experiments the current density depended on the oxalic acid concentration at all tested anodes also at relatively high concentrations.

It was previously shown that the *ICE* for an AO process can be described, in the case of a process not kinetically limited by mass transfer, by the following general expression:[45,46]

$$ICE = \frac{1}{1 + [RH]^*/[RH]^b} \quad (6)$$

where $[RH]^b$ is the concentration of the organic in the bulk and $[RH]^*$ is the value of $[RH]^b$ which gives a current density for the organic oxidation equals to that for the oxygen evolution (e.g. $ICE = 0.5$). $[RH]^*$ can be estimated for each oxidation route (direct oxidation, oxidation by hydroxyl radicals and by adsorbed oxygen) by proper fitting of experimental data,[45,46] and it is a quite simple and effective parameter to evaluate both the efficacy of an anode and the resistance of an organic to AO. In particular, the lower is the value of $[RH]^*$, the fastest is the oxidation of the organic. Hence, the experimental data

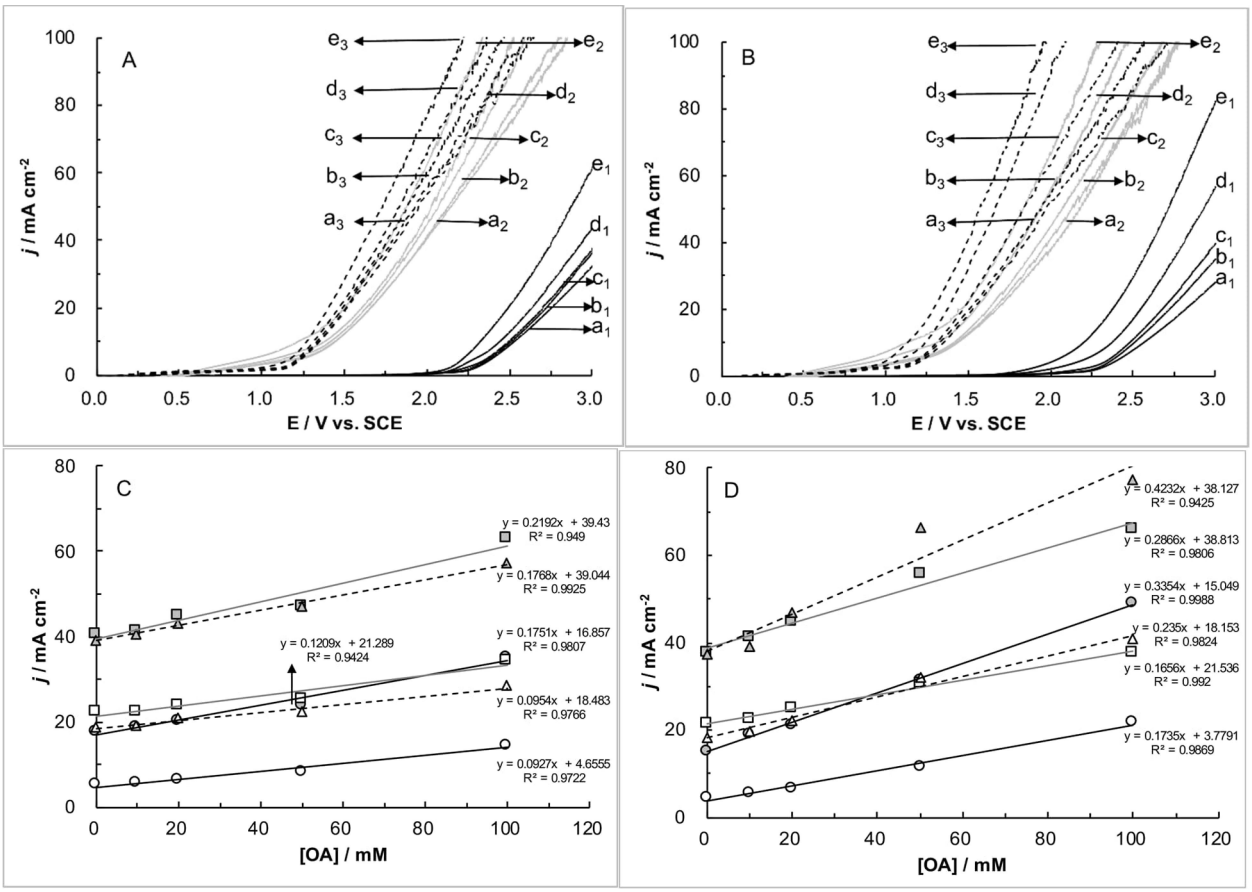

Figure 2. Current density–potential curves for the BDD (–; a_1-e_1)), Ti_4O_7 (---; a_2-e_2), Ti/IrO_2–Ta_2O_5 (- - -; a_3-e_3) electrode at pH of 2 (2 A) and 12 (2B) in the presence of different amounts of oxalic acid: (a) 0 mM; (b) 10 mM; (c) 20 mM; (d) 50 mM; and (e) 100 mM. Plot of current density vs. [OA] at pH of 2 (2 C) and 12 (2D) at different potential values: BDD (2.4 V vs. SCE (○) and 2.7 V vs. SCE (●)), Ti_4O_7 (1.7 V vs. SCE (□) and 2.0 V vs. SCE (■)), Ti/IrO_2–Ta_2O_5 (1.5 V vs. SCE (△) and 1.8 V vs. SCE (▲)) and relative regression lines. System solvent supporting electrolyte: water, Na_2SO_4.

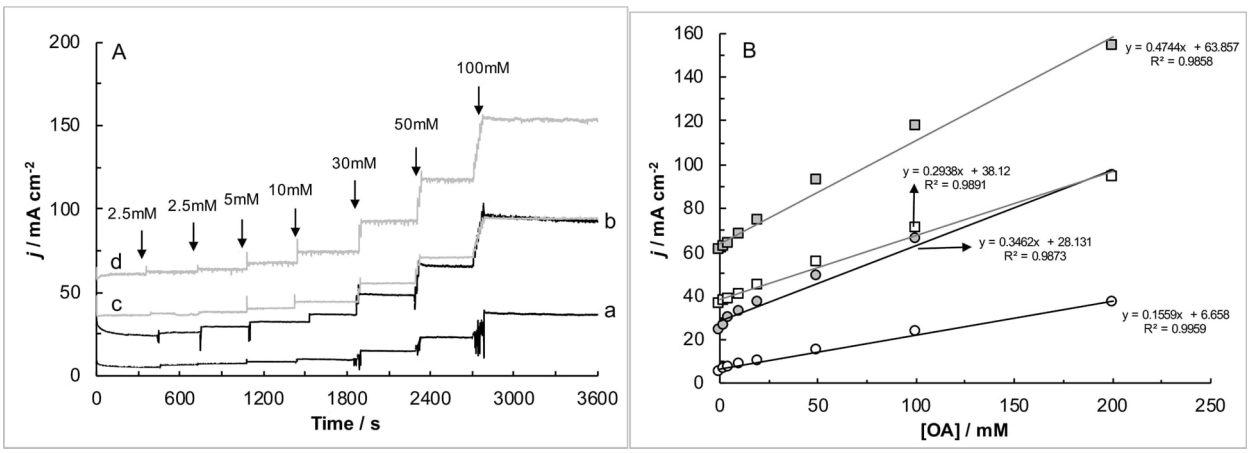

Figure 3. (3 A) Chronoamperometric response of BDD (–) and Ti_4O_7 (---) anode to step-by-step injection of OA at different potentials: BDD (a: 2.4 V vs. SCE (○) and b: 2.7 V vs. SCE (●)), Ti_4O_7 (c: 1.7 V vs. SCE (□) and d: 2.0 V vs. SCE (■)) and (3B) the correspondent current increase as a function of OA concentration. System solvent supporting electrolyte: water, Na_2SO_4.

reported in Figure 1 were used to estimate [*RH*]* as a fitting parameter. As shown in Figure 1, theoretical predictions well fitted experimental data for all the three adopted anodes. In particular, as expected [*RH*]* presented at the IrO_2-based anode a very high value if compared with BDD, while an intermediate situation was observed for Ti_4O_7 (Table 1).

Table 1. Estimation of [*RH*]* for investigated couples organic-anode.[a]

Organic	Anode	[*RH*]*/[mM]
OA	BDD	29
OA	Ti_4O_7	65
OA	$Ti/IrO_2–Ta_2O_5$	100
Phenol	BDD	1.7
Phenol	Ti_4O_7	40
Phenol	$Ti/IrO_2–Ta_2O_5$	300
AO7	BDD	0.5
AO7	Ti_4O_7	37
AO7	$Ti/IrO_2–Ta_2O_5$	110

[a] Values of [*RH*]* estimated by fitting the experimental data in Figures 1, 6 and 7 with theoretical predictions based on eq.s (6) and (7).

Effect of current density

The effect of current density *j* on the AO of OA was previously investigated for many anodes including BDD.[9,26,27] Here, the effect of *j* was evaluated for Ti_4O_7 carrying out a series of galvanostatic electrolyses with 300 rpm at 5, 8.5, 14, 35 and 50 mA cm^{-2} and an initial concentration of OA of 30 mM. For the sake of comparison, the effect of *j* was evaluated also for BDD, the most promising anode, by carrying out some amperostatic experiments under the same operative conditions at 5, 14 and 35 mA cm^{-2}. As shown in Figure 4A and 4D, the higher was *j* the faster was the removal of OA at both Ti_4O_7 and BDD, thus allowing to increase the productivity of the plant (e.g. the volume of water treated with the same cell in a fixed time). As an example, at Ti_4O_7 after 3 hours the increase of the current density from 5 to 50 mA cm^{-2} resulted in an enhancement of the X_{OA} from 24 to 73 %. However, for the same values of *j*, a faster abatement was always achieved at BDD anode. As an example, at 35 mA cm^{-2}, a removal of OA close to 78 and 93 % was achieved after 3.3 h at Ti_4O_7 and BDD, respectively. It is worth to mention that for rather high values of *j* of 35 mA cm^{-2} a further enhancement of the *j* resulted in a quite low increase of X_{OA} due to the fact that, at these high *j*, the process was strongly limited by the mass transfer of the

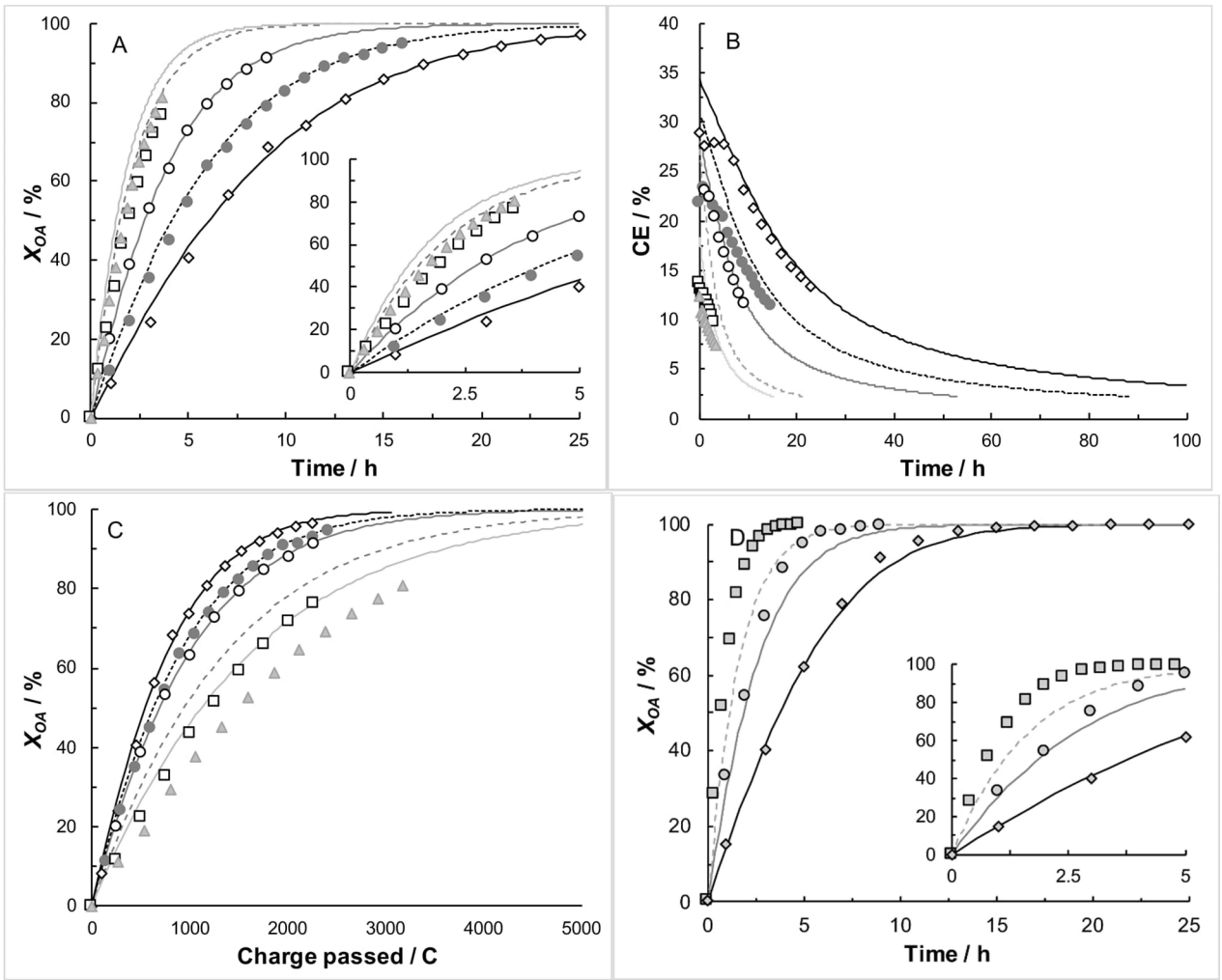

Figure 4. Effect of current density on the X_{OA} (%) (4 A and 4 C) and *CE* (%) (4B) using Ti_4O_7 anode. Electrolyses of a solution of OA (30 mM), Na_2SO_4 (50 mM) (pH 2) were performed at 5 (◇), 8.5 (●), 14 (○), 35 (□), and 50 (▲) mA cm^{-2} and 300 rpm. Ni was used as cathode. The inset in figure 4A shows a zoom on the x-axis within a range time between 0 and 5 hours. Effect of the current density on the X_{OA} (%) (4D) using BDD anode. Electrolysis were performed at 5 (♦), 14 (●), and 35 (■) mA cm^{-2} and 300 rpm. Ni was used as cathode. The inset in figure 4D shows a zoom on the x-axis within a range time between 0 and 5 hours. Theoretical curves (lines) obtained by Eq. (7) with the parameters *[RH]** reported in Table 1

organic to the anodic surface (Figure 4A). More in general, the increase of *j* resulted in all the cases in a decrease of *CE* (Figure 4B) since the oxidation of organics was more limited by the mass transfer rate of OA to the anodic surface while the oxygen evolution fully benefited for the larger working potential caused by higher *j*. Hence, as shown in Figure 4C, the higher was *j* the lower was X_{OA} for the same amount of charge passed. As an example, after 2270 C a removal of 69 and 96% was obtained at 50 and 5 mA cm^{-2}, respectively. According to the literature,[29,38,45] the effect of *j* could potentially be predicted by a suitable theoretical model that considers a process under a mixed kinetic control of the mass transfer of the organic to the anodic surface and of its oxidation reaction using the value of *[RH]** estimated for a process under oxidation reaction control (Figure 1 and Table 1) and the mass transfer coefficient K_m estimated by independent tests (see experimental section) by the following equation:

$$ICE = \frac{1}{1 + \frac{2[RH]^*}{[RH]' + ([RH]'^2 + 4[RH]^* \cdot [RH]^b)^{0.5}}} \quad (7)$$

where $[RH]' = [RH]^b - [RH]^* - C^*$ and $C^* = j/n F K_m$.

It is worth to mention that this theoretical model used in a fully predictive mode allowed to estimate with a quite good accuracy the effect of *j* for both Ti_4O_7 and BDD as shown in Figure 4. In particular, as illustrated in Figure 4B, the theoretical model well captured the effect of the *j* on the *CE*. As an example, for electrolyses carried out at 5 mA cm^{-2} after 7 h the model predicted a value of *CE* of 28% while an experimental value of 26% was achieved; similarly, for electrolyses carried out at 35 mA cm^{-2} for 5.5 h the model gave a final value of *CE* of 6% such as the experiment.

Effect of mixing rate and of the initial concentration of OA

Two very important parameters for AO are the mixing rate and the concentration of the organics. Indeed, the mixing rate affects the mass transfer of the organic to the anodic surface, thus influencing the performances of the oxidation of organics when it is under the kinetic control of the mass transfer stage or under a mixed kinetic regime.[45] Moreover, a higher concentration of the organic from one hand accelerates its oxidation but from the other hand requires a larger amount of charge and time passed to achieve the same residual value of organic concentration. The effect of the mixing rate was here evaluated for the Ti_4O_7 anode carrying out a series of galvanostatic electrolyses at 8.5, 14 and 35 mA cm^{-2} and 0, 300 and 700 rpm with an initial concentration of OA of 30 mM. As shown in Table 2 and in Figure 5, the enhancement of mixing rate resulted in a faster removal of OA, thus allowing to increase the productivity of the plant (e.g. the volume of water treated with the same cell in a fixed time), and in a higher *CE*, because of the faster mass transfer of OA to the anodic surface. As an example, the increase of mixing rate from 0 to 700 rpm gave an increase of the final X_{OA} from 86 to 98% at 8.5 mA cm^{-2} and from 64 to 77% at 35 mA cm^{-2}.

Table 2. Effect of mixing rate at different current densities.[a]

Current density/ [mA cm^{-2}]	Mixing rate/ [rpm]	Time passed/ [h]	Charge passed /[C]	Final abatement/ [%]	Final *CE*/[%]
8.5	0	15	2268	86	11.0
8.5	300	15	2268	93	11.9
8.5	700	15	2268	98	12.5
14	0	9	2268	74	9.4
14	300	9	2268	91	11.6
14	700	9	2268	93	12
35	0	3.6	2268	64	8.2
35	300	3.6	2268	72	8.4
35	700	3.6	2268	77	9.8

[a] Anode: Ti_4O_7; Cathode: Ni; Pollutant: Oxalic acid (30 mM).

In particular, the fastest abatement (96% after 4.8 h) was achieved using the highest adopted values of both *j* (35 mA cm^{-2}) and mixing rate (700 rpm) (Figure 5C). More in general, the data reported in Table 2 confirms that an increase of *j* gives rise to higher X_{OA} and lower *CE* at all adopted mixing rates.

Figure 5 reports the experimental data of X_{OA} vs. time for the tested *j* and mixing rates and the corresponding predictions of the theoretical model based on eq. (7). It is worth to mention that the model well predicted the coupled effect of mixing rate and *j* for most of experimental data.

The effect of the initial concentration of OA was studied by a series of electrolyses carried out using Ti_4O_7 as anode, Ni as cathode, a mixing rate of 300 rpm, a *j* of 14 mA cm^{-2} and three different initial concentrations of OA (namely, 10.6, 32 and 73 mM). As shown in Figure 6B, the higher was the initial concentration the higher were both the experimental and theoretical *CE* of the process that show quite similar values. Indeed, as previously mentioned, the increase of concentration of the organic accelerates both the oxidation reaction rate (see eq. (5) as an example) and its mass transfer rate to the anode surface. However, as shown in Figure 6A a longer time (and a higher amount of charge passed) is required to achieve similar final values when a higher initial concentration of OA is present. As an example, to achieve a final value lower than 3 mM of OA, 5, 9 and 10 hours were necessary for experiment performed with an initial concentration of OA of 11, 32 and 73 mM.

Effect of the nature of organic

It has been shown several times that the performances of AO can strongly depend on both the anode and the nature of the organic pollutant. Hence, we performed a series of electrolysis using three anodes (Ti_4O_7, BDD and Ti/IrO_2–Ta_2O_5) and three different organic pollutants: oxalic acid, phenol and Acid Orange 7 (AO7), which are all characterized by a quite high resistance to oxidation processes. Electrolyses with phenol and AO7 were carried out using a Ni cathode, 300 rpm and 8.5 mA cm^{-2}. As shown in Figure 7A, at Ti/IrO_2–Ta_2O_5 a negligible abatement of phenol was achieved after 2300 C (close to 2–3%), thus conforming the very high resistance of this

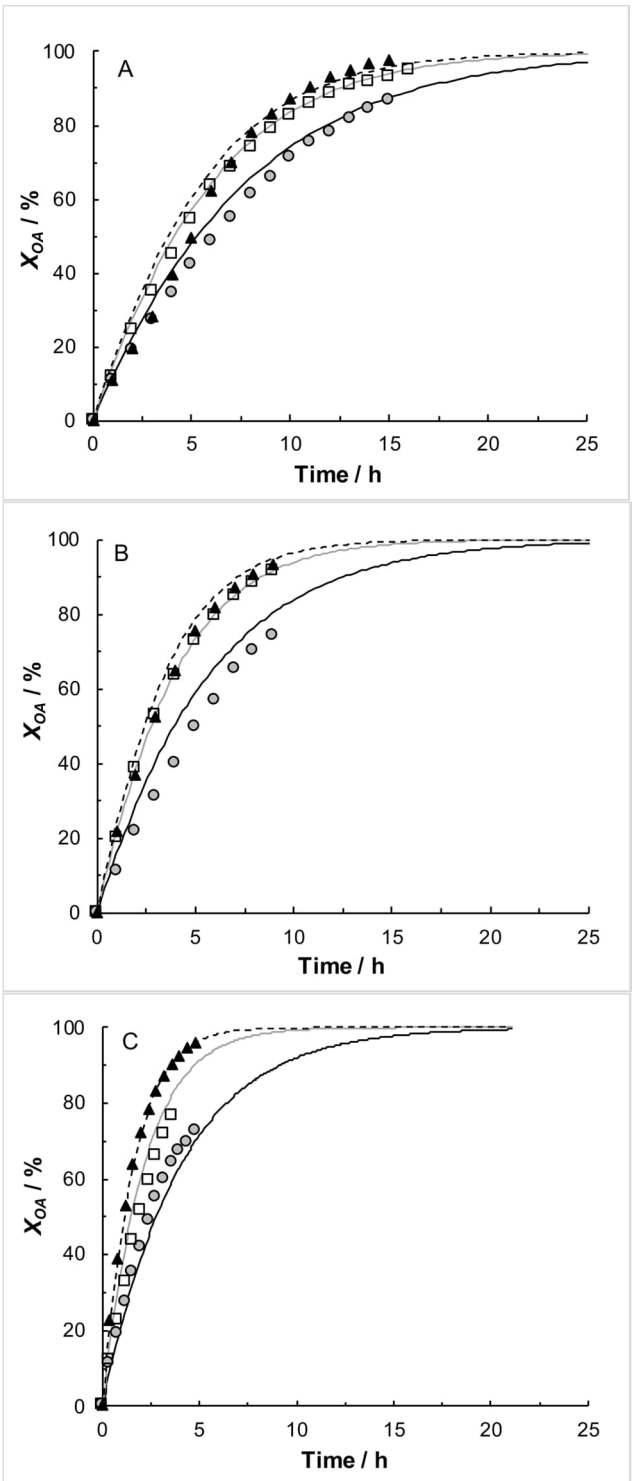

Figure 5. Effect of the mixing rate on the X_{OA} (%) at 8.5 (5 A), 14 (5B), and 35 (5 C) mA cm^{-2}. Electrolyses were performed with a solution of OA (30 mM), Na_2SO_4 (50 mM) (pH 2) under different mixing: 0 (●), 300 (□), and 700 (▲) rpm. Ti_4O_7 and Ni were used as anode and cathode, respectively. Theoretical curves (lines) obtained by Eq. (7) with the parameters *[RH]** reported in Table 1.

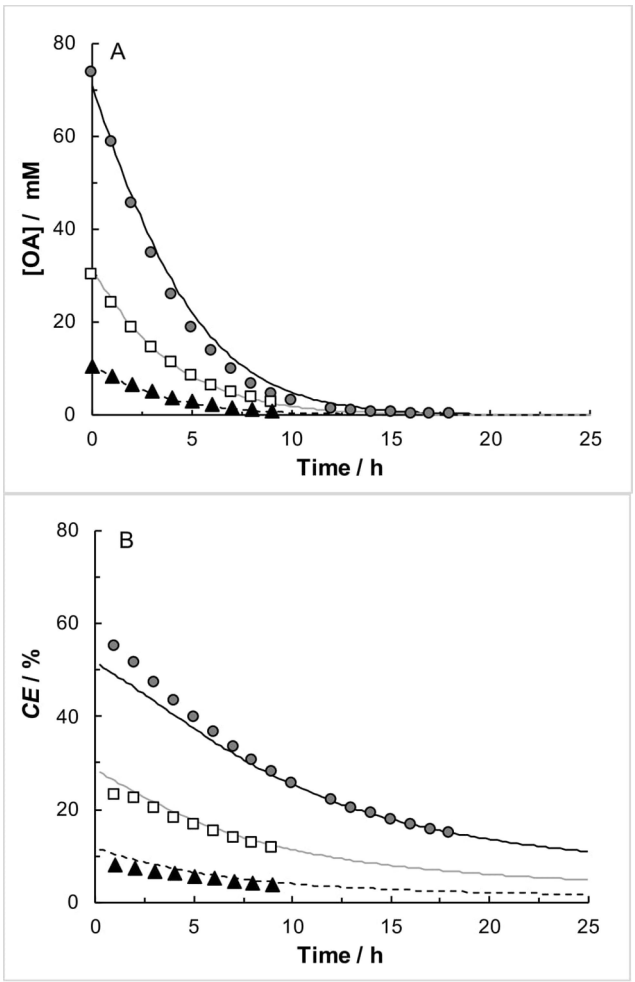

Figure 6. Plot of concentration of [OA] (6 A) and *CE* (%) (6B) vs. time passed. Electrolysis were performed at 14 mA cm^{-2} and 300 rpm with a solution of OA at different initial concentration values, Na_2SO_4 (50 mM)(pH 2). Initial OA concentration: 73 (●), 31 (□), and 10.6 (▲) mM. Ti_4O_7 and Ni were used as anode and cathode, respectively. Theoretical curves (lines) obtained by Eq. (7) with the parameters *[RH]** reported in Table 1.

molecule to oxidation processes. Conversely, when BDD anode was used, a very high removal of phenol was obtained (100% after 6 h and 907 C), as a result of the very high reactivity of hydroxyl radicals generated at this anode. An intermediate situation arises for Ti_4O_7; indeed, in this case at the end of the electrolysis (15 h and 2268 C) a removal of about 50% was obtained. It is well known that the anodic oxidation of phenolic compounds proceed through the formation of many intermediates and, in particular, of different carboxylic acids that are particularly resistant to AO and that are often mineralized at longer times with respect to that required for the disappearance of the starting organic.[1,2] Indeed, as shown in Figure 7B, for the same amount of charge passed, a lower abatement of TOC occurred with respect to the abatement of phenol for both BDD and Ti_4O_7. As an example, at BDD anode after 600 C an abatement of phenol and TOC close to 98 and 72% were achieved, respectively. This difference is caused by the presence in the solution of many intermediates including oxalic, maleic, tartaric, malonic and fumaric acids. However, as shown in Figure 7C (which reports the overall concentration of carboxylic acids vs. the charge passed) and 7D (which reports the

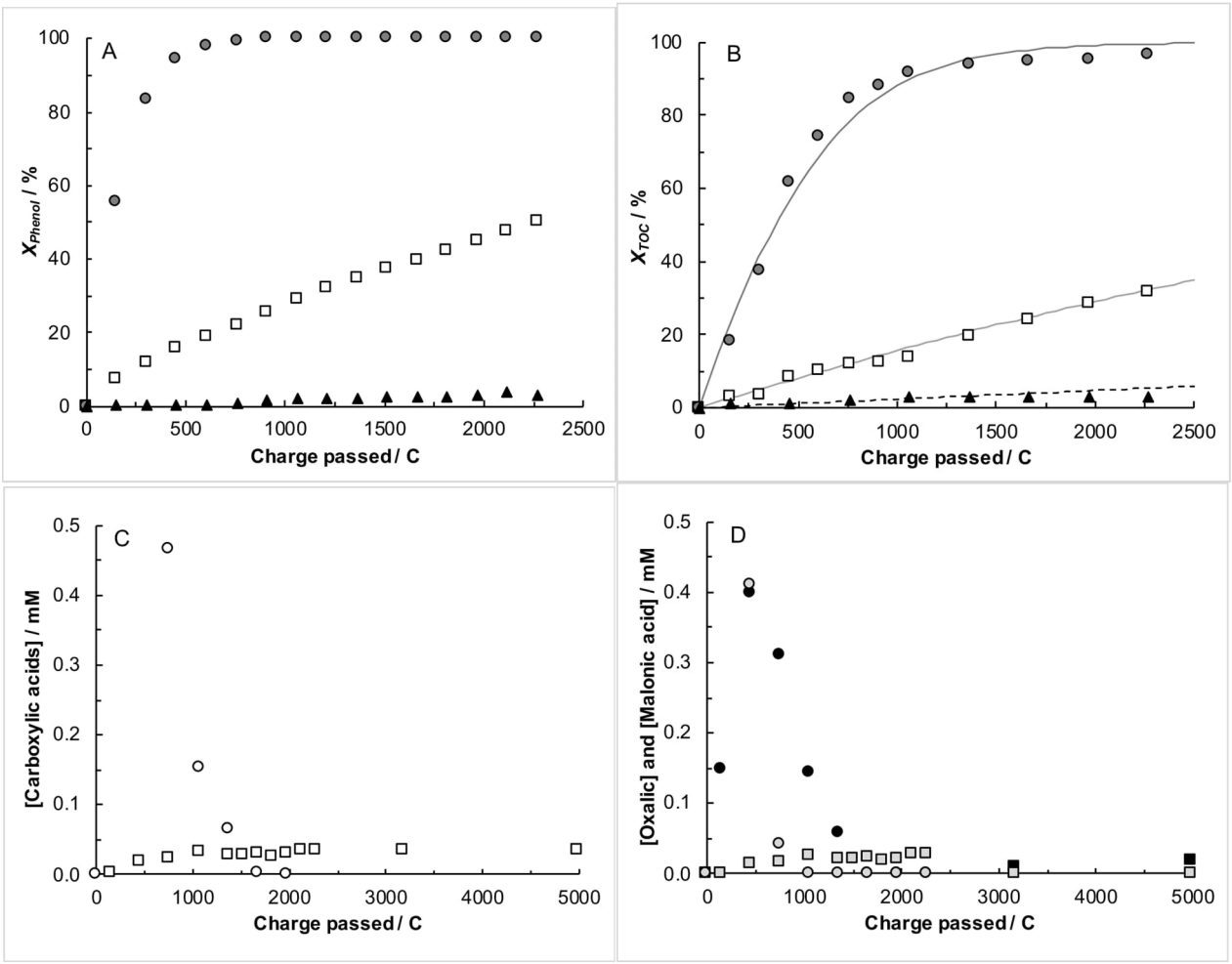

Figure 7. Effect of the nature of the anode BDD (●), Ti_4O_7 (□) or Ti/IrO_2–Ta_2O_5 (▲) on the X_{Phenol} (%) (7 A) and X_{TOC} (%) (7B). Electrolyses of a solution of phenol (2.5 mM), Na_2SO_4 (50 mM) (pH 2) were performed at 8.5 mA cm^{-2} and 300 rpm. Ni was used as cathode. Figure 6C reports the overall concentration of detected carboxylic acids (BDD/Ti_4O_7 ○/□) while Figure 7D the concentrations of Oxalic (BDD/Ti_4O_7 ●/■) and Malonic acids (BDD/Ti_4O_7 ●/■) vs. charge passed.

concentrations of malonic and oxalic acids) in the second part of the electrolysis all these carboxylic acids were removed, and the removal of TOC reached a final value close to 96% (Figure 7B). Also, in the case of Ti_4O_7, the removal of TOC was lower with respect to that of phenol. However, both the formation and the removal of carboxylic acids were slower with respect to BDD as a result of a less effective oxidation of phenol. As an example, after 1000 C a plethora of carboxylic acids was detected for BDD for a total concentration close to 0.5 mM while for Ti_4O_7 only quite large maleic and malonic acids were observed for a total concentration close to 0.03 mM. Conversely, after 2268 C no carboxylic acids and phenol were observed at BDD while phenol, maleic and malonic acids were still present at Ti_4O_7 and oxalic acid was formed at this anode only after 3000 C (Figure 7D). By prolonging the electrolysis at Ti_4O_7 up to 5000 C a decrease of the concentration of carboxylic acids was observed (Figure 7C and 7D). However, phenol (removal close to 70%) and oxalic acid were still present, and the removal of TOC was lower than 60% as a result of a quite low current efficiency close to 3%.

In addition, under these adopted operative conditions, after 15 h and 2268 C, the EC per g_{TOC} using Ti_4O_7 for the phenol removal was approximately 0.75 kWh/g_{TOC}, which is 2.8 times higher with respect to the BDD (~0.25 kWh/g_{TOC}) and more than 11 times lower than that of Ir-based anode (~7.76 kWh/g_{TOC}), thus showing that Ti_4O_7-based anode could be appealing from the perspective of the applicative scale with respect to both BDD and Ir-based anode for the phenol removal.

In the case of AO7, a quite high removal of the concentration of the organic pollutant was achieved at all the tested anodes (Figure 8A); indeed, after 1000 C a removal of AO7 higher than 94% was obtained at both BDD, Ti_4O_7 and Ti/IrO_2–Ta_2O_5. However, a very different picture was obtained for the removal of TOC (Figure 8B). Indeed, after 2268 C a removal of TOC of 100, 15 and 6% was achieved at BDD, Ti_4O_7 and Ti/IrO_2–Ta_2O_5, respectively, because of very large differences in the *CE* (14, 2 and 0.6% at BDD, Ti_4O_7 and Ti/IrO_2–Ta_2O_5, respectively). Also in the case of AO7, after 2268 C, the usage of Ti_4O_7 give rise to an intermediate value of EC per g_{TOC} of approximately of 2.20 kWh/g_{TOC} (~0.30 and 11.5 kWh/g_{TOC} for

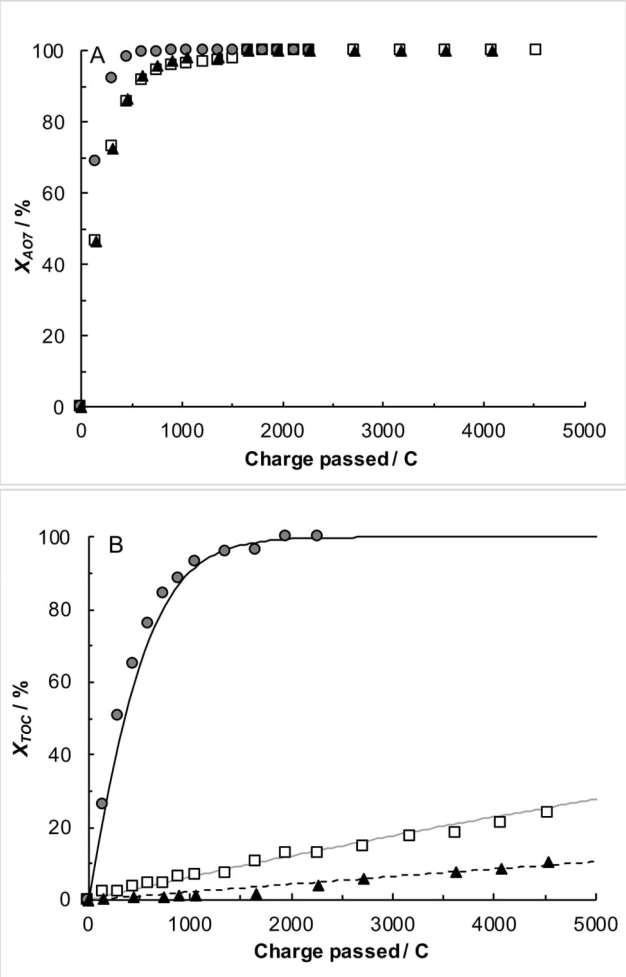

Figure 8. Effect of the anode BDD (●), Ti_4O_7 (□) or Ti/IrO_2–Ta_2O_5 (▲) on the X_{AO7} (%) (8 A) and X_{TOC} (%) (8B). Electrolyses of a solution of AO7 (0.8 mM), Na_2SO_4 (50 mM) (pH 2) were performed at 8.5 mA cm^{-2} and 300 rpm. Ni was used as cathode.

BDD and Ti/IrO_2–Ta_2O_5, respectively). When electrolyses were prolonged up to 4500 C a removal of TOC of 10 and 24% was obtained at Ti/IrO_2–Ta_2O_5 and Ti_4O_7, respectively, as a result of the presence in the solutions of many intermediates such as various carboxylic acids (formic, acetic, lactic and fumaric ones). In particular, in the experiments performed with Ti_4O_7 the carboxylic acid with the highest concentration was acetic acid which is known to be particularly resistant to AO processes.[43]

In order to better evaluate the relative ability of the adopted anodes for the mineralization of OA, AO7 and phenol, the experimental data for TOC removal were fitted by the theoretical model presented in the previous paragraphs with the aim to estimate the values of [*RH*]*. The estimated values of [*RH*]* at BDD, Ti_4O_7 and Ti/IrO_2–Ta_2O_5 electrodes for OA, AO7 and phenol were reported in Table 1. It is observed that BDD, which gives rise to the anodic formation of very reactive hydroxyl radicals, presents very low values of [*RH*]*, especially for OA and phenol. Conversely, for Ti/IrO_2–Ta_2O_5, where chemisorbed oxygen is likely to be involved in the oxidation process, very high values of [*RH*]* were always observed, while intermediate values were observed for Ti_4O_7.

Conclusion

In this study, the performance of anodic oxidation of wastewater contaminated by recalcitrant organic pollutants was investigated using Ti_4O_7 as anode and oxalic acid, phenol, and Acid Orange 7 as model organic compounds. Moreover, the performances of Ti_4O_7 were compared with that of BDD and Ti/IrO_2–Ta_2O_5 anodes. It was found that Ti_4O_7 presents intermediate values of both the abatement of the organic pollutant and of TOC and of current efficiency with respect to BDD, which always presented the best performances, and Ti/IrO_2–Ta_2O_5 for the abatement of all investigated compounds. In the case of oxalic acid, at the end of the electrolysis, an abatement of ~99 and ~94% was achieved using BDD and Ti_4O_7, respectively, while Ti/IrO_2–Ta_2O_5 gave a lower abatement close to 84% at 5 mA cm^{-2} and 300 rpm.

Moreover, it was found that it is possible to improve the results of the anodic oxidation at Ti_4O_7 using suitable values of the current density and of the mixing rate. In particular, Ti_4O_7 allows to reach the fastest abatement of oxalic acid up to 96% after 4.8 h using the highest adopted values of both current density (35 mA cm^{-2}) and mixing rate (700 rpm).

In the case of phenol, Ti_4O_7 gave intermediate performances with respect to BDD and Ti/IrO_2–Ta_2O_5 anodes. In particular, after 2268 C, a removal of about 50% of phenol and 31% of TOC were obtained using Ti_4O_7 at 300 rpm and 8.5 mA cm^{-2}. Furthermore, by prolonging the electrolysis up to 5000 C, a removal of phenol close to 70% and of TOC lower than 60% was observed, as a result of the presence of many carboxylic acids, such as malonic and oxalic acid in the solution, which were formed during the electrolysis.

In the case of Acid Orange 7, Ti_4O_7 shows the same performances on the abatement of the pollutant for all the investigated anodes; after 1000 C a removal of Acid Orange 7 higher than 94% was obtained using both BDD, Ti_4O_7 and Ti/IrO_2–Ta_2O_5 at 300 rpm and 8.5 mA cm^{-2}. Conversely, a removal of TOC of 100% using BDD after 2268 C, 24 and 10% using Ti_4O_7 and Ti/IrO_2–Ta_2O_5 after 4500 C, respectively, was observed, as a result of the formation of quite resistant carboxylic acids. In the case of Ti_4O_7, acid acetic was identified as the main organic in solution.

Eventually, it was shown that the performances of the process at Ti_4O_7 can be described by a theoretical model previously developed for other anodes with a good agreement between theoretical predictions and experimental data. In particular, the model was able to predict without the addiction of tunable fitting parameters the effect of current density, mixing rate and initial concentration of the organic.

Experimental Section

Electrolyses were performed in an undivided glass cell with magnetic stirring equipped with a Ti_4O_7 (Deqing Chuangzhi Technology Co.,Ltd), BDD (Condias) or Ti/IrO_2–Ta_2O_5 (commercial DSA®, De Nora SpA) anode with a wet surface close to 3.5 cm^2 and a Ni (Carlo Erba Reagents) cathode. The volume of solution was 50 mL. Electrolyses were performed with amperostatic alimentation (Amel 2053 potentiostat/galvanostat) at room temperature. Most of the experiments were repeated at least twice, giving rise to a good reproducibility of results (±4%). Bi-distilled water and Acid Orange 7 0.80 mM (Sigma Aldrich), oxalic acid 30 mM (Sigma Aldrich) or phenol 2.45 mM (Merck) were used as received as solvent and model pollutants, respectively. Na_2SO_4 50 mM (Janssen Chimica) was used as supporting electrolyte to enhance the conductivity of the solution. H_2SO_4 (Sigma Aldrich) and NaOH (Sigma Aldrich) were used to adjust the pH. The total organic carbon (TOC) was analyzed by a TOC-L CSH/CSN analyzer Shimadzu. The concentration of oxalic acid and other carboxylic acids was evaluated by HPLC using an Agilent 1260 fitted with a Rezex ROA-Organic Acid column (Phenomenex) at 25 C° and coupled with a UV detector working at 210 nm. A water solution 0.005 N of H_2SO_4 (Sigma Aldrich) was eluted at 0.5 mL min^{-1} as the mobile phase. The concentration of phenol was evaluated by HPLC using an Agilent 1260 fitted with a Kinetex 5u C18 column (Phenomenex) at 25 C° and coupled with a UV detector working at 214 nm. A solution of water (Honeywell, HPLC grade) and acetonitrile (Merck, HPLC grade) was eluted at 1 mL min^{-1} as the mobile phase. It was used a gradient type elution. In particular, the gradient profile was: *i*) time = 0 min 20/80 $\%_{vol/vol}$ acetonitrile/water; *ii*) time = 5 minutes 95/5 $\%_{vol/vol}$ acetonitrile/water. Calibration curves were obtained by using the pure standards of carboxylic acids (purity > 99%, Sigma Aldrich), and phenol (purity > 99%, Merck). The abatement (e.g., the conversion) of the total organic carbon (X_{TOC}) and the current efficiency for the removal of the TOC (CE_{TOC}) were defined by Eqs. (8) and (9), respectively.

$$X_{TOC} = (\Delta TOC)_t / TOC^\circ \quad (8)$$

$$CE_{TOC} = n\ F\ V\ C^\circ X_{TOC} / I\ t \quad (9)$$

where (ΔTOC)t is the decay of the TOC ($mg_{carbon}\,L^{-1}$), TOC° and C° the initial concentrations of the TOC ($mg_{carbon}\,L^{-1}$) inside the electrochemical cell, respectively, *n* is the number of electrons exchanged for the oxidation of the organic pollutant to carbon dioxide (84 for the AO7, 28 for phenol and 2 for OA, respectively), *F* the Faraday constant (96487 C mol^{-1}), *I* the applied current intensity, *t* the electrolysis time and *V* the volume of the cell. The instantaneous current efficiency is given by:

$$ICE_{TOC} = n\ F\ V\ \Delta C / I\ \Delta t \quad (10)$$

The abatement (e.g., the conversion) of the oxalic acid (X_{AO}) or phenol (X_{phenol}) or Acid Orange 7 (X_{AO7}) and the current efficiency (*CE*) were defined by Eqs. (11) and (12), respectively.

$$X_{AO\ (phenol,\ AO7)} = (C_{\ AO\ (phenol,\ AO7)})_t / C^\circ_{\ AO\ (phenol,\ AO7)} \quad (11)$$

$$CE = n\ F\ V\ C^\circ\ X_i / I\ t \quad (12)$$

where $C_{\ AO\ (phenol,\ AO7)t}$ and $C^\circ_{AO\ (phenol,\ AO7)}$ are the decay and the initial concentration of the oxalic acid, phenol or Acid Orange 7, respectively, *n* is the number of electrons exchanged for the oxidation of the organic pollutant to carbon dioxide (84 for the AO7, 28 for phenol and 2 for OA, respectively).

Energetic consumption was computed by following eq. (13).

$$EC = I^* \Delta V\ t / g_{TOC}\ (or\ Kg_{TOC\text{-}eq}) \quad (13)$$

where g_{TOC} *and* $Kg_{TOC\text{-}eq}$ are respectively TOC value removed during the electrolysis and the TOC equivalent removed considering that all the mole of oxalic acid was mineralized to CO_2 and H_2O.

The thickness of the stagnant layer in the adopted conditions was estimated trough a typical limiting-current essay using the redox couple hexacyanoferrate(II)/hexacyanoferrate(III) focusing on the oxidation reaction and using the value 6.631×10^{-10} $m^2\,s^{-1}$ for the diffusivity of ferry-cyanide ion,[47] BDD as anode and Ni as cathode. The mass transfer coefficient of oxalic acid k_m was estimated as the ratio between the diffusivity of oxalic acid *D* and the thickness of the stagnant layer, where *D* was assumed to be 1.1×10^{-9} $m^2\,s^{-1}$.[48,49]

Acknowledgements

University of Palermo is acknowledged for its financial support. Open Access Funding provided by Universita degli Studi di Palermo within the CRUI-CARE Agreement.

Conflict of Interest

The authors declare that they have no known competing financial interests or personal relationships that could have appeared to influence the work reported in this paper.

Data Availability Statement

The data that support the findings of this study are available from the corresponding author upon reasonable request.

Keywords: Anodic Oxidation · BDD · Ti_4O_7 · Toxic organic compounds · wastewater treatment

[1] C. A. Martínez-Huitle, M. A. Rodrigo, I. Sirés, O. Scialdone, *Chem. Rev.* **2015**, *115*, 13362–13407.
[2] C. A. Martínez-Huitle, O. Scialdone, M. A Rodrigo, *Electrochemical Water and Wastewater Treatment Elsevier* **2018**.
[3] C. A. Martìnez-Huitle, M. Panizza, *Curr. Opin. Electrochem.* **2018**, *11*, 62–71.
[4] O. Scialdone, *Electrochim. Acta* **2009**, *54*, 6140–6147.
[5] Y. He, H. Lin, Z. Guo, W. Zhan, H. Li, W. Huang, *Sep. Purif. Technol.* **2019**, *212*, 802–821.
[6] O. Scialdone, F. Proietto, A. Galia, *Curr. Opin. Electrochem.* **2021**, *27*, 100682.
[7] Y. Hao, H. Ma, F. Proietto, A. Galia, O. Scialdone, *Electrochim. Acta* **2022**, *402*,139480.
[8] E. Brillas, I. Sirés, M. A. Oturan, *Chem. Rev.* **2009**, *109*, 6570–6631.
[9] P. Ma, C. Prestigiacomo, F. Proietto, A. Galia, O. Scialdone, *ChemElectroChem* **2021**, *8*, 3135–3142.
[10] P. Ma, X. Hao, F. Proietto, A. Galia, O. Scialdone, *Electrochim. Acta* **2020**, *354*,136733.
[11] P. Ma, X. Hao, A. Galia, O. Scialdone, *Chemosphere* **2020**, *248*, 125994.
[12] S. Sabatino, A. Galia, G. Saracco, O. Scialdone, *ChemElectroChem* **2017**, *4*, 150–159.
[13] D. Clematis, M. Panizza, *Curr. Opin. Electrochem.* **2021**, *30*, 100844.

[14] O. Scialdone, A. Galia, C. Guarisco, S. Randazzo, G. Filardo, *Electrochim. Acta* **2008**, *53*, 2095–2108.
[15] G. Chen, E. A. Betterton, R. G. Arnold, *J. Appl. Electrochem.* **1999**, *29*, 961–970.
[16] O. Scialdone, A. Galia, G. Filardo, *Electrochim. Acta* **2008**, *53*, 7220–7225.
[17] P. Geng, J. Su, C. Miles, C. Comninellis, G. Chen, *Electrochim. Acta* **2015**, *153*, 316–324.
[18] S. O. Ganiyu, N. Oturan, S. Raffy, M. Cretin, R. Esmilaire, E. Hullebusch, G. Esposito, M. A. Oturan, *Water Res.* **2016**, *106*, 171–182.
[19] S. O. Ganiyu, N. Oturan, S. Raffy, M. Cretin, C. Causserand, M. A. Oturan, *Sep. Purif. Technol.* **2019**, *208*, 142–152.
[20] H. Lin, J. Niu, S. Liang, C. Wang, Y. Wang, F. Jin, Q. Qi, Q. Huang, *Chem. Eng. J.* **2018**, *354*, 1058–1067.
[21] D. Zhi, J. Wang, Y. Zhou, Z. Luo, Y. Sun, Z. Wan, L. Luo, D. D. W. Tsang, D. D. Dionysiou, *Chem. Eng. J.* **2020**, *383*, 123149.
[22] A. M. Zaky, B. P. Chaplin, *Environ. Sci. Technol.* **2014**, *48*, 5857–5867.
[23] N. Oturan, S. O. Ganiyu, S. Raffy, M. A. Oturan, *Appl. Catal. B* **2017**, *217*, 214–223.
[24] F. C. Walsh, R. G. A. Wills, *Electrochim. Acta* **2010**, *55(22)*, 6342–6351.
[25] D. Bejan, E. Guinea, N. J. Bunce, *Electrochim. Acta* **2012**, *69*, 275–281.
[26] D. Gandini, E. Mahé, P. A. Michaud, W. Haenni, A. Perret, C. Comninellis, *J. Appl. Electrochem.* **2000**, *30*, 1345–1350.
[27] C. A. Martınez-Huitle, S. Ferro, A. De Battisti, *Electrochim. Acta* **2004**, *49*, 4027–4034.
[28] P. Canizares, J. Garcia-Gomez, J. Lobato, M. A. Rodrigo, *Ind. Eng. Chem. Res.* **2003**, *42*, 956–962.
[29] O. Scialdone, A. Galia, C. Guarisco, S. Randazzo, G. Filardo, *Electrochim. Acta* **2008**, *53*, 2095–2108.
[30] O. Scialdone, S. Randazzo, A. Galia, G. Filardo, *Electrochim. Acta* **2009**, *54*, 1210–1217.
[31] O. Scialdone, A. Galia, S. Randazzo, *Chem. Eng. J.* **2011**, *174*, 266–274.
[32] J. Zhi, H. Wang, T. Nakashima, T. Rao, A. Fujishima, *J. Phys. Chem. B.* **2003**, *107*, 13389–13395.
[33] O. Scialdone, A. Galia, S. Sabatino, *Appl. Catal. B* **2014**, *148–149*, 473–483.
[34] M. Panizza, P. A. Michaud, G. Cerisola, Ch. Comninellis, *J. Electroanal. Chem.* **2001**, *507*, 206–214.
[35] P. Canizares, J. Garcia-Gomez, J. Lobato, M. A. Rodrigo, *Ind. Eng. Chem. Res.* **2004**, *43*, 1915–1922.
[36] A. M. Polcaro, M. Mascia, S. Palmas, A. Vacca, *Ind. Eng. Chem. Res.* **2002**, *41*, 2874–2881.
[37] O. Scialdone, A. Galia, C. Guarisco, S. Randazzo, G. Filardo, *Electrochim. Acta* **2008**, *53*, 2095–2108.
[38] O. Scialdone, *Electrochim. Acta* **2009**, *54*, 6140–6147.
[39] O. Scialdone, A. Galia, S. Randazzo, *Chem. Eng. J.* **2012**, *183*, 124–134.
[40] C. Comninellis, *Electrochim. Acta* **1994**, *39*, 1857–1862.
[41] J. Willsau, J. Heitbaum, *Electrochim. Acta.* **1986**, *31*, 943–948.
[42] S. Fierro, T. Nagel, H. Baltruschat, C. Comninellis, *Electrochem. Commun.* **2007**, *9*, 1969–1974.
[43] O. Scialdone, A. Galia, C. Guarisco, *Electrocatalysis* **2013**, *4*, 290–301.
[44] F. Ross, A. B. Ross, *In selected specific rates of reactions of transients from water in aqueous solutions*, **1977**, 20234.
[45] O. Scialdone, A. Galia, In *Synthetic Diamond Films: Preparation, Electrochemistry, Characterization, and Applications* **2011**, 261–280.
[46] O. Scialdone, A. Galia, C. Guarisco, S. La Mantia, *Chem. Eng. J.* **2012**, *189–190*, 229–236.
[47] C. A. Martinez-Huitle, S. Ferro, A. De Battisti, *J. Appl. Electrochem.* **2005**, *35*, 1087–1093.
[48] J. Kulas, I. Roušar, J. Jirkovský, *J. Appl. Electrochem.* **1998**, *28*, 843–853.
[49] M. Ciszkowska, Z. Stojek, J. G. Osteryoung, *J. Electroanal. Chem.* **1995**, *398*, 45.

Manuscript received: January 3, 2022
Revised manuscript received: February 15, 2022
Accepted manuscript online: February 18, 2022